



CUE2015-Applied Energy Symposium and Summit 2015: Low carbon cities and urban energy systems

## Impact of guide wall geometry on the power output of a solar chimney power plant

Siyang Hu<sup>a</sup>, Dennis Y.C. Leung<sup>a,\*</sup>

<sup>a</sup>*Department of Mechanical Engineering, the University of Hong Kong, Pokfulam, Hong Kong, China*

---

### Abstract

This study investigated the impact from the geometry of guide walls (GWs) on the power output of a solar chimney power plant. Numerical simulations found a reduction in the mass flow rate after adding a guide wall in the system. The driving force and the velocity, however, showed a significant increase along the increasing altitude of GWs. The potential maximum power output was enlarged by 29.6% in a cylindrical-chimney system and by 6.3% in a divergent-chimney system compared to the system without guide walls. Based on the results, the GW height should be a primary criterion for designing GWs.

© 2016 The Authors. Published by Elsevier Ltd. This is an open access article under the CC BY-NC-ND license (<http://creativecommons.org/licenses/by-nc-nd/4.0/>).

Peer-review under responsibility of the organizing committee of CUE 2015

*Keywords:* Solar chimney, Guide wall, Power output, CFD

---

### 1. Introduction

Solar chimney power plant (SCPP) is a system that converts solar thermal energy into electricity by generating a buoyant updraft inside a chimney to drive wind turbines. SCPP has advantages in its low cost in operation and its capability of providing clean energy without aggravating environmental pollution and intensifying climate change. It is believed that there is a high application potential of SCPP in developing countries that have large available lands and abundant solar insolation [1]. Recently, novel concepts has been proposed in which SCPP would be assembled with heat exchangers in the collector or hot exhaust injection in the chimney [2, 3]. By this, the new SCPP systems could utilize solar energy as well as the waste heat from industries, especially the low grade waste heat stored in cooling water or hot exhaust gas

---

\* Corresponding author. Tel.: +852 2858 5415; fax: +852 2859 7911.  
*E-mail address:* [ytleung@hku.hk](mailto:ytleung@hku.hk).

stream, which may improve the efficiency of urban energy systems such as thermal power plants, and hence reduce their carbon emissions.

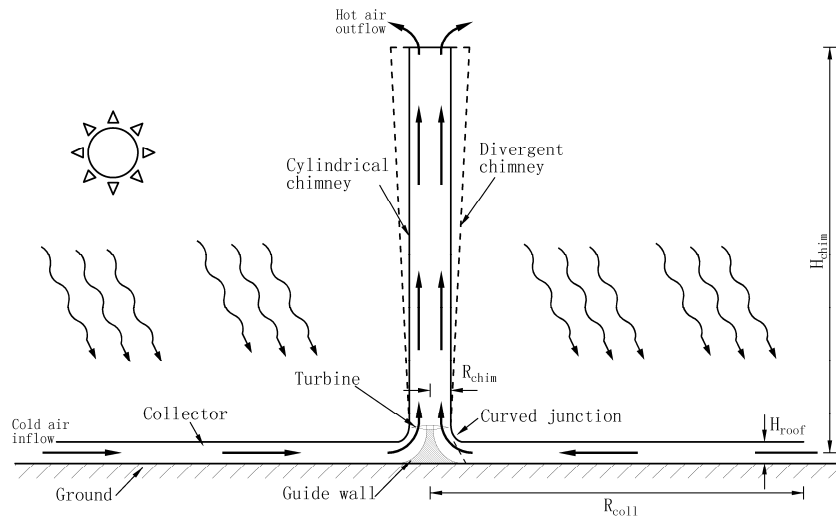


Fig. 1. The guide wall subset (in shadow) locates below the chimney entrance and holds the blades of the turbine.

Studying the impact of the geometry of components in a solar chimney is a primary task. Much attention has been paid to the chimney and the collector [4-7]. The critical roles of design variables, e.g. collector diameter, chimney height, solar radiation and other ambient conditions, to determine the system power output have been widely discussed [4-10]. Guide wall (GW), a component in the collector-to-chimney transition region, is also a prominent subset as it can be used to assist the horizontal air flow in shifting to the updraft and be the holder of the turbine (as shown in Fig. 1). Individual studies revealed the potential impact of the GW on the buoyant flow by examining the systems with and without such a component, which indicated that this subset would be capable of modifying the velocity of the flow and thus significantly affect the performance of SCPP [4, 5]. However, the detailed knowledge on the aerodynamic features of GWs is ambiguous and quantitative evaluation of its impact on the system performance is still uncertain. In other words, it is unknown how the detail geometric parameters, e.g. the height or the radius of GWs, affect the buoyant flow in the system. Therefore, it would be difficult to optimize the geometry of GWs.

In this study, the investigation on GWs was further extended by CFD simulations with GWs with different heights and radiuses. Therefore, variation in the flow in SCPP induced by the modification in the two geometric parameters (i.e. height and radius) were respectively discussed based on the numerical outcomes. By this, we can evaluate the influence from different parameters and identify the critical factors in relation to the aerodynamic features of GWs. Meanwhile, the GWs were coupled to a cylindrical chimney as well as a divergent chimney as some articles found a remarkable improvement of the flow velocity in divergent chimneys [7, 11]. Thus, we have expected different reactions from the divergent-chimney SCPP when the GW configurations varied.

## 2. Methodology

### 2.1. The physical model in simulation

As Manzanares power plant is the only large-scaled SCPP in the world, the simulated solar chimney was based on its dimensions, i.e. 195m in chimney height and 244 m in collector diameter. Based on the original cylindrical chimney with a radius in 5m, the divergent chimney was acquired by just increasing the exit radius to 10m.

The geometry of the GWs are as follows: (1) for investigating the impact of GW height, the height varied from 2m to 12m in an interval of 2m with a fixed radius in 13.2m; and (2) for studying the impact of radius, the radius increased from 2.8m to 13.2m in an interval of 2.6m while the height remained at 10m. For identifying different configurations, each configuration was labeled by GW-HxRy: ‘GW’ stands for ‘Guide Wall’, ‘Hx’ stands for the wall height in ‘x’ meters and ‘Ry’ stands for the wall foot radius in ‘y’ meters.

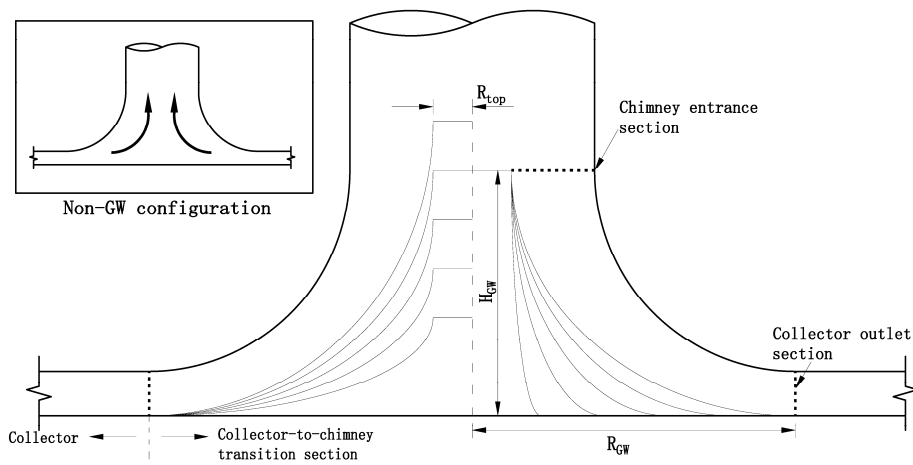


Fig. 2. Configurations of the guide wall with a fixed radius in 13.2m (left half plane); configurations with a fixed height in 10m (right half plane). Inset diagram at the left-top is the configuration without GW.

### 2.2. Numerical model and other settings in simulation

Based on its dimensions, the flow in a SCPP should be fully turbulent [12]. Thus, the equations of the conservation of momentum, energy and mass were adjusted into RANS form and coupled with standard k-ε model as shown below.

Continuity equation

$$\frac{\partial(\rho u)}{\partial x} + \frac{\partial(\rho v)}{\partial y} = 0 \quad (1)$$

Navier-Stokes equation

$$\frac{\partial(\rho u u)}{\partial x} + \frac{\partial(\rho u v)}{\partial y} = \rho g \beta (T - T_{\infty}) + \mu \left( \frac{\partial^2 u}{\partial x^2} + \frac{\partial^2 u}{\partial y^2} \right) \quad (2)$$

$$\frac{\partial(\rho v u)}{\partial x} + \frac{\partial(\rho v v)}{\partial y} = -\frac{\partial(p)}{\partial y} + \mu \left( \frac{\partial^2 v}{\partial x^2} + \frac{\partial^2 v}{\partial y^2} \right) \quad (3)$$

Energy conservation equation

$$\frac{\partial(\rho u C_p T)}{\partial x} + \frac{\partial(\rho v C_p T)}{\partial y} = \lambda \left( \frac{\partial^2 T}{\partial x^2} + \frac{\partial^2 T}{\partial y^2} \right) \quad (4)$$

k-ε model

$$\frac{\partial(\rho k u_i)}{\partial x_i} = \frac{\partial}{\partial x_i} \left( \left( \mu + \frac{\mu_t}{\sigma_k} \right) \frac{\partial k}{\partial x_j} \right) + G_k + G_b - \varepsilon \rho + S_k \quad (5)$$

$$\frac{\partial(\rho \varepsilon u_i)}{\partial x_i} = \frac{\partial}{\partial x_j} \left( \left( \mu + \frac{\mu_t}{\sigma_\varepsilon} \right) \frac{\partial \varepsilon}{\partial x_j} \right) + C_{1\varepsilon} (G_k + C_{3\varepsilon} G_b) - C_{2\varepsilon} \rho \frac{\varepsilon^2}{k} + S_\varepsilon \quad (6)$$

These equations governed the flow in the axisymmetric and steady-state simulation and solved by ANSYS FLUENT 14.0 with the boundary conditions described in Table 1.

The potential power output of the system can be calculated by the mathematical model as follows [13]:

$$P_{out} = x \cdot \sqrt{1-x} \cdot \eta_t \cdot \Delta p \cdot \frac{\dot{m}}{\rho_0} \quad (7)$$

We can obtain the maximum extractable power output of the system by making  $x$  equal to  $2/3$  [13]. The coefficient of turbine,  $\eta_t$ , was set to 80% in this study. The driving force of the whole system,  $\Delta p$ , was approximately equal to the absolute value of the area-weighted averaged gauge pressure at the chimney entrance acquired from the numerical outcomes.

Table 1. Details of boundary conditions

Surface	Value
Collector roof	$T_{ext} = 302 \text{ K}$ , $h_s = 10 \text{ W/m}^2\text{K}$ , $\varepsilon_{ext} = 0.89$
Soil bottom	$T = 302 \text{ K}$
Soil lateral sides	Adiabatic
Chimney shell	Adiabatic free-slip
GW surface	Adiabatic free-slip
Ground	$Q = 720 \text{ W/m}^3$ ; <i>Thickness</i> = 0.0001 m
Collector inlet	$T_{ext} = 302 \text{ K}$ , $p_{gauge} = 0 \text{ Pa}$
Chimney exit	$T_{ext} = 300 \text{ K}$ , $p_{gauge} = 0 \text{ Pa}$

### 2.3. Validity

Case GW-H10R13.2 was used to evaluate the validity of our numerical model as its dimension was fairly close to the scenario of the SSCP in Manzanares. The simulated velocity was 16.4 m/s, which is 7.4% higher than the measurement ( $\sim 15 \text{ m/s}$ ) mainly due to the overestimation of the air temperature rise,  $\Delta T$  (21.8 K V.S. 20 K). Considering the uncertainties in soil properties and the adiabatic assumption at the solid boundaries, the accuracy of our model was acceptable for the subsequent study.

### 3. Results and discussion

#### 3.1. Effect of GW height

Fig. 3 and 4 indicated the effect of GW heights on different parameters (i.e. mass flow rate, driving force, velocity, temperature and power output). The air temperature at the chimney entrance section showed little changes when the wall height increased from 0m to 12m. The slight difference was meant to induce consistency in the buoyant flow, but the driving force (i.e. the absolute value of the gauge pressure at chimney entrance section) and the velocity at the chimney entrance section had an evident increase with increasing the GW height. For instance, the GWs, with height larger than 8m, enlarged the driving force by 14.0 - 40.7Pa, namely 10-30% higher than the case of GW-H0 in the cylindrical-chimney group. In the divergent-chimney group, GW -H4 and -H6 slightly diminished the driving force while the force increased by 6.0%, 11.9% and 12.1% with the 8m-, 10m- and 12m- high walls, respectively. Moreover, a downside in the mass flow rate following the increasing heights was identified in Fig. 3 and Fig. 4. However, the cylindrical chimney had less decline in the mass flow rate while the drop reached 24-231 kg/s, i.e. 1-8% less than the zero GW configuration in the divergent-chimney system.

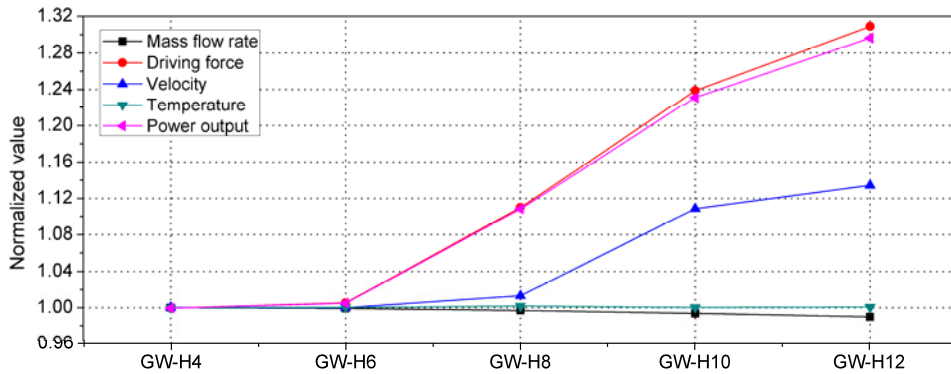


Fig. 3. Variations in the potential of the cylindrical-chimney system along with GW heights. Normalized by GW-H0 case.

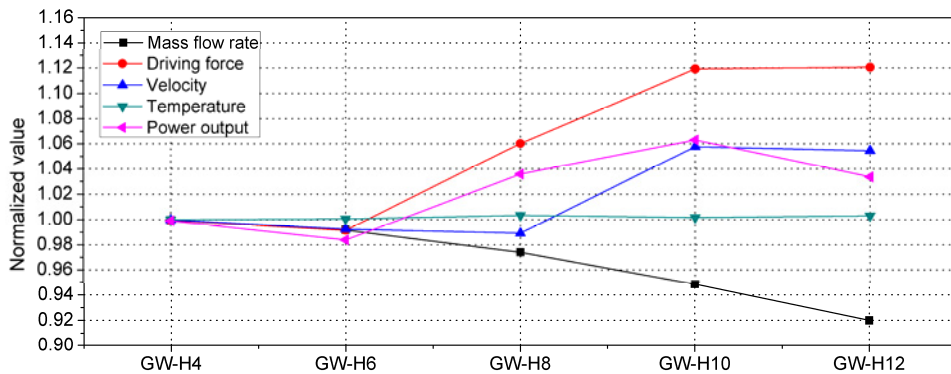


Fig. 4. Variations in the potential of the divergent-chimney system along with GW heights. Normalized by GW-H0 case.

The maximum extractable power output is the product of the driving force and the mass flow rate as shown in Eqn. (7). As the mass flow rate varied little in the cylindrical group, the power output was mainly improved by the enlarged driving force. GW -H8, -H10 and -H12 improved the power output by 6kW (10.8%), 12kW (23.1%) and 15kW (29.8%) respectively. As to the divergent group, the power output of GW- H4 and H6 was even lower than the GW-H0 case due to the decline in both the mass flow rate and the driving force. Even the driving force was significantly enlarged under GW -H8 to -H12 configurations, the lower mass flow rate restricted the improvement in the power output. Consequently, the peak power output acquired in the divergent-chimney group was only 6.7% higher than that in the GW-H0 case.

### 3.2. Effect of GW radius

Figs. 5 and 6 indicated the effect of varying radius on different parameters. The lines in the figures were almost horizontal indicating slight variations in all of the parameters when the radius varied from 2.8m to 13.2m. The difference between the cases with and without the GWs (the lines were obviously above 1.0) should not be caused by the radius but by the height of GWs. In other words, the impact from GWs radius on the system performance was much weaker than the height.

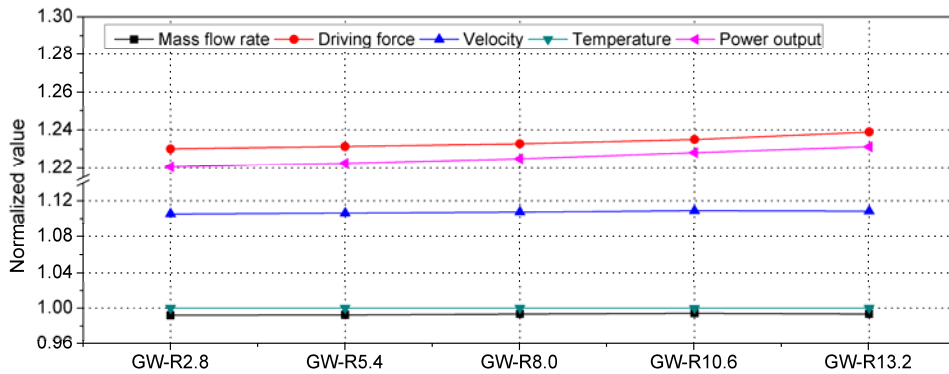


Fig. 5. Variations in the potential of the cylindrical-chimney system along with GW radius. Normalized by GW-H0 case.

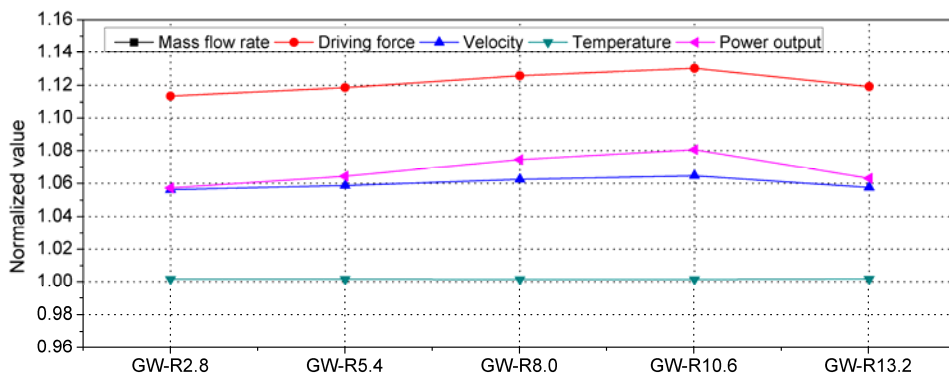


Fig. 6. Variations in the potential of the divergent-chimney system along with GW radius. Normalized by GW-H0 case.

In addition to that, the tendency in the divergent-chimney system differed from that in the cylindrical-chimney system. Instead of the continually but slightly increasing tendency in the cylindrical chimney, the driving force and the power output in the divergent-chimney system increased at the beginning but started to drop when the radius exceeded 10.6m.

#### 4. Conclusion

In this study, we have examined the effect of geometry of GWs on the performance of a SCPP by numerical simulations.

A reduction in mass flow rate was found in the numerical outcomes after adding GWs into the system, which approximately had a linear relationship with the GW height but was almost independent of the modification in the radius. On the other hand, the driving force and the velocity were significantly improved by the GWs in both the cylindrical-chimney and divergent-chimney system, and mainly affected by the GW heights as well. As the potential power output is mainly governed by the driving force, the improvement in the power output was fairly similar to the tendency in the driving force enhancement. Furthermore, as expected, the divergent-chimney system showed different reactions to the geometry of GWs compared to the cylindrical-chimney system. Following these results, the GW height should be a primary criterion in a practical plant design of GWs.

#### Acknowledgements

This project is funded by the CRCG grant of the University of Hong Kong.

#### References

- [1] Schlaich J. *The solar chimney: electricity from the sun*. Edition Axel Menges; 1995.
- [2] Zandian A, Ashjaee M. The thermal efficiency improvement of a steam Rankine cycle by innovative design of a hybrid cooling tower and a solar chimney concept. *Renewable Energy* 2013;**51**:465-73.
- [3] Ghorbani B, Ghashami M, Ashjaee M. Electricity production with low grade heat in thermal power plants by design improvement of a hybrid dry cooling tower and a solar chimney concept. *Energy Conversion and Management* 2015;**94**:1-11.
- [4] dos Santos Bernardes MA, Molina Valle R, Cortez MF-B. Numerical analysis of natural laminar convection in a radial solar heater. *International journal of thermal sciences* 1999;**38**:42-50.
- [5] Ming T, Liu W, Xu G. Analytical and numerical investigation of the solar chimney power plant systems. *International Journal of Energy Research* 2006;**30**:861-73.
- [6] Serag-Eldin MA. Analysis of effect of geometric parameters on performance of solar chimney plants. *ASME Summer Heat Transfer Conference, San Francisco, CA, United states: American Society of Mechanical Engineers*; 2005, p. 587-95.
- [7] Ming T, Richter RK, Meng F, Pan Y, Liu W. Chimney shape numerical study for solar chimney power generating systems. *International Journal of Energy Research* 2013;**37**:310-22.
- [8] Ming T, Wang X, De Richter RK, Liu W, Wu T, Pan Y. Numerical analysis on the influence of ambient crosswind on the performance of solar updraft power plant system. *Renewable and Sustainable Energy Reviews* 2012;**16**:5567-83.
- [9] Ming T, Gui J, de Richter RK, Pan Y, Xu G. Numerical analysis on the solar updraft power plant system with a blockage. *Solar Energy* 2013;**98**:58-69.
- [10] Pretorius JP, Kroger DG. Critical evaluation of solar chimney power plant performance. *Solar Energy* 2006;**80**:535-44.
- [11] Koonsrisuk A, Chitsomboon T. Effects of flow area changes on the potential of solar chimney power plants. *Energy* 2013;**51**:400-6.

[12] Pastohr H, Kornadt O, Gürlebeck K. Numerical and analytical calculations of the temperature and flow field in the upwind power plant. *International Journal of Energy Research* 2004;**28**:495-510.

[13] Koonsrisuk A, Chitsomboon T. Mathematical modeling of solar chimney power plants. *Energy* 2013;**51**:314-22.



### **Biography**

Prof. Dennis Y.C. Leung received his Ph.D in 1988 from the Department of Mechanical Engineering at the University of Hong Kong. He joined the same department in 1993 and is now a full professor of the department specializing in renewable energy and energy conservation. He has published more than 400 articles including 210+ peer reviewed SCI journal papers. Prof. Leung is one of the top 1% highly cited scholars in energy field from 2010 to 2014.